

Article

# Hadron–Quark Phase Transition in the SU (3) Local Nambu–Jona-Lasinio (NJL) Model with Vector Interaction

Grigor Alaverdyan 

Department of Radio Physics, Yerevan State University, 1 Alex Manoogian Street, Yerevan 0025, Armenia; galaverdyan@ysu.am

**Abstract:** We study the hadron–quark hybrid equation of state (EOS) of compact-star matter. The Nambu–Jona-Lasinio (NJL) local SU (3) model with vector-type interaction is used to describe the quark matter phase, while the relativistic mean field (RMF) theory with the scalar-isovector  $\delta$ -meson effective field is adopted to describe the hadronic matter phase. It is shown that the larger the vector coupling constant  $G_V$ , the lower the threshold density for the appearance of strange quarks. For a sufficiently small value of the vector coupling constant, the functions of the mass dependence on the baryonic chemical potential have regions of ambiguity that lead to a phase transition in nonstrange quark matter with an abrupt change in the baryon number density. We show that within the framework of the NJL model, the hypothesis on the absolute stability of strange quark matter is not realized. In order to describe the phase transition from hadronic matter to quark matter, Maxwell’s construction is applied. It is shown that the greater the vector coupling, the greater the stiffness of the EOS for quark matter and the phase transition pressure. Our results indicate that the infinitesimal core of the quark phase, formed in the center of the neutron star, is stable.

**Keywords:** quark matter; NJL model; RMF theory; deconfinement phase transition; Maxwell construction



**Citation:** Alaverdyan, G. Hadron–Quark Phase Transition in the SU (3) Local Nambu–Jona-Lasinio (NJL) Model with Vector Interaction. *Symmetry* **2021**, *13*, 124. <https://doi.org/10.3390/sym13010124>

Received: 26 November 2020

Accepted: 8 January 2021

Published: 13 January 2021

**Publisher’s Note:** MDPI stays neutral with regard to jurisdictional claims in published maps and institutional affiliations.



**Copyright:** © 2021 by the author. Licensee MDPI, Basel, Switzerland. This article is an open access article distributed under the terms and conditions of the Creative Commons Attribution (CC BY) license (<https://creativecommons.org/licenses/by/4.0/>).

## 1. Introduction

The study of the thermodynamic properties and constituent composition of strongly interacting matter at extremely high density/temperature is important for understanding many phenomena both in microscopic and macroscopic worlds. Many regularities in the region of low densities and high temperatures can be obtained from experiments of heavy-ion collisions. In the region of extremely high densities and low temperatures, compact stars are the main source that enriches our understanding about the structure of the matter [1–4]. It is known that the macroscopic properties of compact stars have a functional dependence on the equation of state of matter in a wide range of densities, starting from the density of ordinary matter of atomic-molecular composition to values tens of times higher than the nuclear density at which various exotic structures can appear, such as the pion condensate, kaon condensate, deconfined quark phase, and color superconducting phase.

Theoretical studies of the observable macroscopic parameters (e.g., mass, radius, moment of inertia, surface gravitational redshift) of the static configurations of compact stars and a comparison with the results of observations make it possible to refine the equation of state of superdense matter and exclude those that contradict the observational data obtained for most of the existing models of the equation of state. Some dynamical manifestations can stand for an observational test confirming or refuting the existence of deconfined quark matter in the interior of compact stars. The thermal evolution of compact stars is an example of such a process [5,6]. Another observational manifestation of a quark phase transition is an abrupt change in the stellar radius, when the accretion of matter onto the star increases the central pressure to a critical value, resulting in a quark core being formed in the center of the star [7].

Over the past several decades, numerous works have appeared devoted to the theoretical study of the thermodynamic properties of deconfined quark matter and the elucidation of the possibility of its presence in the central part of compact stars. Research in this area became more intense after the discovery of the pulsars PSR J1614-2230 [8] and PSR J0348 + 0432 [9], which have a mass of about two solar masses. The existence of neutron stars with such masses indicates the stiffness of the equation of state for compact-star matter. The absence of a unified rigorous theory that would allow the equation of state (EoS) of strongly interacting matter to be calculated in this wide range of density values leads to the need of using different models for describing the properties of matter in both hadronic and deconfined quark phases.

In many works, the authors have combined the phenomenological MIT bag model [10] for quark matter with various models for hadronic matter to obtain a hybrid EoS and, on its basis, have investigated the properties of quark–hadron hybrid stars (see, e.g., [11–22]). The MIT quark bag model was also used to study the properties of so-called strange stars [23–30], the existence of which is associated with the Bodmer-Witten-Terazawa-Itoh hypothesis of the absolute stability of strange quark matter in relation to ordinary nuclear matter [31–34].

Recently, the Nambu–Jona-Lasinio (NJL) model [35,36] was used very often to describe the quark matter. The NJL model, which was first proposed to explain the origin of the nucleon mass by considering spontaneous chiral symmetry breaking, was later reformulated to describe quark matter. This model successfully reproduces many features of quantum chromodynamics (QCD) [37–41]. By combining various modifications of the NJL quark model with different models for describing hadronic matter, the authors of a number of works have constructed a hybrid equation of state and, on their basis, have investigated the properties of neutron stars containing deconfined quark matter (see, e.g., [42–52]). Several approaches for studying the properties of both quark matter and hadronic matter and, on their basis, elucidating the features of the quark–hadron phase transition can be found in the topical issue [53].

It was shown in Ref. [54] that the inclusion of a repulsive vector-interaction term helps in producing high-mass neutron stars. The results of Refs. [18,19,55] have shown that in the relativistic mean field (RMF) model, taking into account the  $\delta$ -meson effective field increases the stiffness of the EOS for hadronic matter.

The aim of this work is to obtain a hybrid EOS of strongly interacting matter within the framework of a model in which the quark component is considered in the local SU (3) NJL model including the vector interaction term; meanwhile, hadronic matter is described in the framework of the RMF model, taking into account the contribution of the scalar-isovector  $\delta$ -meson field. Due to the uncertainties in the value of the vector coupling constant  $G_V$  of quarks, different values of this constant are considered and the changes in the parameters of the first-order phase transition, caused by the different vector interaction strengths, are clarified.

The main distinguishing features of this work compared to the already existing works devoted to the study of the hybrid equation of state of stellar matter are as follows. For the hadronic phase, we applied the extended RMF model, in which, in addition to other exchange meson fields, the contribution of the scalar-isovector  $\delta$ -meson field is also taken into account. This leads to a stiffer EOS for the hadronic component, which is important for modeling compact stars with a high mass. By considering quark matter in the extended NJL model, in which vector coupling is also taken into account, we determine the threshold for the appearance of  $s$ -quarks in beta-equilibrium quark matter, and investigate the dependence of this threshold on the vector coupling strength. This will allow, in the future, to consider the possibility of the existence of two-layer quark stars in the central part, of which there is a core of quark matter with strangeness, surrounded by nonstrange quark matter. The problem of the validity of Witten’s hypothesis about the absolute stability of strange quark matter in the framework of the NJL model is also examined. Within the framework of the model considered here, we also discuss the fulfillment of the stability

condition for an infinitely small core of a quark phase newly formed in the center of a compact star.

The paper is organized as follows. In Section 2, we describe the SU (3) local NJL model with scalar and vector couplings for deconfined quark matter, and present the computational results for thermodynamic quantities of cold three-flavor quark matter in  $\beta$ -equilibrium. In Section 3, we describe the RMF model with a  $\delta$ -meson effective field for hadronic matter in  $\beta$ -equilibrium. In Section 4, we study the constant pressure phase transition (Maxwell scenario) from hadronic matter to quark matter, and construct the EOS of compact star matter for different values of the vector coupling constant. Finally, in Section 5, we summarize and discuss our findings from this work.

## 2. Quark Matter Phase

### 2.1. Local SU (3) NJL Model with a Vector Interaction Term

In order to describe the deconfined quark matter, we use the local three-flavor Nambu–Jona-Lasinio (NJL) model. The Lagrangian density within the local SU (3) NJL model, including the terms of both scalar and vector interactions, has the following form:

$$\begin{aligned} \mathcal{L}_{NJL} = & \bar{\psi}(i\gamma^\mu\partial_\mu - \hat{m}_0)\psi + G_S \sum_{a=0}^8 \left[ (\bar{\psi}\lambda_a\psi)^2 + (\bar{\psi}i\gamma_5\lambda_a\psi)^2 \right] \\ & - K \left\{ \det_f(\bar{\psi}(1 + \gamma_5)\psi) + \det_f(\bar{\psi}(1 - \gamma_5)\psi) \right\} - G_V \sum_{a=0}^8 \left[ (\bar{\psi}\gamma_\mu\lambda_a\psi)^2 + (\bar{\psi}i\gamma_\mu\gamma_5\lambda_a\psi)^2 \right] \end{aligned} \quad (1)$$

Here,  $\psi$  represents quark spinor fields  $\psi_f^c$  with three flavors  $f = u, d, s$  and three colors  $c = r, g, b$ . The first term is the Dirac Lagrangian density of free quark fields with the current quark mass matrix  $\hat{m}_0 = \text{diag}(m_{0u}, m_{0d}, m_{0s})$ . The second term corresponds to the chiral-symmetric four-quark interaction with the coupling constant  $G_S$ , where  $\lambda_a (a = 1, 2, \dots, 8)$  are Gell–Mann matrices and SU(3) group generators in the flavor space, and  $\lambda_0 = \sqrt{2/3}\hat{I}$  ( $\hat{I}$  is the identity  $3 \times 3$  matrix). The third term corresponds to the six-quark Kobayashi–Maskawa–’t Hooft [56] interaction with the coupling constant  $K$ , which leads to the axial  $U_A(1)$  symmetry breaking. This interaction is important for obtaining the mass splitting between pseudoscalar isosinglet mesons  $\eta'(958)$  and  $\eta(547)$ . It is thanks to this term in the chiral limit ( $m_{0u} = m_{0d} = m_{0s} = 0$ ) that the  $\eta'$  meson mass grows to a finite value, while other pseudoscalar mesons, including  $\eta$ , remain massless. Inclusion of this interaction term in the Lagrangian makes it possible to reproduce the mass values of the  $\eta$  and  $\eta'$  mesons within the framework of the NJL model. The fourth term represents the vector and axial-vector channels of interaction with a positive coupling constant  $G_V$ .

In some works (see, e.g., [40,57]), in order to involve the vector coupling in the expression for the NJL Lagrangian density, the flavor-singlet-vector ( $\omega$ -type) term,  $\mathcal{L}_V = -G_V^{(0)}(\bar{\psi}\gamma_\mu\lambda_0\psi)^2$ , is added. There are works that use a term  $\mathcal{L}_V = -G_V^{(8)}\sum_{a=1}^8(\bar{\psi}\gamma_\mu\lambda_a\psi)^2$  corresponding to the flavor-octet-vector coupling ( $\rho$ -type). In Refs. [50–52], the unification of these two approaches is considered, and the term

$$\mathcal{L}_V = -G_V^{(0)}(\bar{\psi}\gamma_\mu\lambda_0\psi)^2 - G_V^{(8)}\sum_{a=1}^8(\bar{\psi}\gamma_\mu\lambda_a\psi)^2$$

is included based on the assumption that the vector coupling constants  $G_V^{(0)}$  and  $G_V^{(8)}$ , in the general case, can have different values. As the value of vector coupling constants are unknown, these values are considered as free parameters of the model. In this work, following Refs. [58–60], we considered the constants  $G_V^{(0)}$  and  $G_V^{(8)}$  to be equal,  $G_V^{(0)} = G_V^{(8)} = G_V$ , which from a physical point of view, means that in a vacuum, the mass degeneracy of  $\omega$  and  $\rho$  mesons takes place [60].

Using the mean field approximation from the Lagrangian (1), we can obtain an expression for the functional part of the density of a thermodynamic grand potential  $\tilde{\Omega}_{NJL}(T, \{M_f\}, \{\tilde{\mu}_f\})$

$$\tilde{\Omega}_{NJL} = -\frac{3}{\pi^2} \sum_{f=u,d,s} \left\{ \int_0^\Lambda dk k^2 \left[ E_f(k, M_f) + T \ln \left( 1 + e^{-\frac{E_f(k, M_f) - \tilde{\mu}_f}{T}} \right) + T \ln \left( 1 + e^{-\frac{E_f(k, M_f) + \tilde{\mu}_f}{T}} \right) \right] \right\} \\ + \sum_{f=u,d,s} \left[ 2G_s \sigma_f(T, M_f, \tilde{\mu}_f)^2 - 2G_V n_f(T, M_f, \tilde{\mu}_f)^2 \right] \\ - 4K \sigma_u(T, M_u, \tilde{\mu}_u) \sigma_d(T, M_d, \tilde{\mu}_d) \sigma_s(T, M_s, \tilde{\mu}_s) \quad (2)$$

where  $\Lambda$  is the momentum ultraviolet cutoff parameter, the need for which arises in connection with the nonrenormalizability of the NJL model;  $E_f(k, M_f) = \sqrt{k^2 + M_f^2}$  is the energy of the quark quasiparticle of flavor  $f$ ; and  $\tilde{\mu}_f$  is expressed through the chemical potential  $\mu_f$  and number density  $n_f$  of a quark of flavor  $f$  as follows:

$$\tilde{\mu}_f = \mu_f - 4G_V n_f. \quad (3)$$

The quark number densities are determined by the expression

$$n_f(T, M_f, \tilde{\mu}_f) = \frac{3}{\pi^2} \int_0^\Lambda dk k^2 \left[ \frac{1}{1 + e^{\frac{E_f(k, M_f) - \tilde{\mu}_f}{T}}} - \frac{1}{1 + e^{\frac{E_f(k, M_f) + \tilde{\mu}_f}{T}}} \right]. \quad (4)$$

In Equation (2), for the thermodynamic potential,  $\sigma_f(T, M_f, \tilde{\mu}_f)$  ( $f = u, d, s$ ) denotes the quark condensates  $\langle \bar{\psi}\psi \rangle$ , which are defined as follows

$$\sigma_f(T, M_f, \tilde{\mu}_f) = \langle \bar{\psi}_f \psi_f \rangle = -\frac{3}{\pi^2} M_f \int_0^\Lambda dk \frac{k^2}{E_f(k, M_f)} \left[ 1 - \frac{1}{1 + e^{\frac{E_f(k, M_f) - \tilde{\mu}_f}{T}}} - \frac{1}{1 + e^{\frac{E_f(k, M_f) + \tilde{\mu}_f}{T}}} \right]. \quad (5)$$

In the mean-field (Hartree) approximation, the gap equations for the constituent quark masses have the form

$$M_u = m_{0u} - 4G_S \sigma_u + 2K \sigma_d \sigma_s, \\ M_d = m_{0d} - 4G_S \sigma_d + 2K \sigma_s \sigma_u, \\ M_s = m_{0s} - 4G_S \sigma_s + 2K \sigma_u \sigma_d. \quad (6)$$

In this work, we assumed (as in many similar works of other authors) that the values of the energy density and pressure in the vacuum are equal to zero. Of course, in this case too, in order to compare it with the MIT bag model, it was also possible to single out the effective bag constant  $B_{eff}$ . However, this would not affect the EOS, which was the main goal of our work. In the future, we intend to investigate a case when the vacuum value of the thermodynamic grand potential is nonzero.

The density of the grand thermodynamic potential corresponding to the quark component is determined by the expression

$$\Omega_{NJL}(T, \{M_f\}, \{\mu_f\}) = \tilde{\Omega}_{NJL}(T, \{M_f\}, \{\mu_f\}) - \tilde{\Omega}_{NJL}(T = 0, \{n_f = 0\}). \quad (7)$$

Denoting the quark condensates and the masses of the constituent quarks in vacuum by  $\sigma_{f0}$  and  $M_{f0}$ , respectively, for the thermodynamic grand potential density of the quark component, one can obtain

$$\Omega_{NJL} = -\frac{3}{\pi^2} \sum_{f=u,d,s} \left\{ \int_0^\Lambda dk k^2 \left[ E_f(k, M_f) + T \ln \left( 1 + e^{-\frac{E_f(k, M_f) - \tilde{\mu}_f}{T}} \right) + T \ln \left( 1 + e^{-\frac{E_f(k, M_f) + \tilde{\mu}_f}{T}} \right) \right] \right\} \\ + \frac{3}{\pi^2} \sum_{f=u,d,s} \int_0^\Lambda dk k^2 E_f(k, M_{f0}) + 2G_s (\sigma_u^2 + \sigma_d^2 + \sigma_s^2 - \sigma_{u0}^2 - \sigma_{d0}^2 - \sigma_{s0}^2) \\ - 4K (\sigma_u \sigma_d \sigma_s - \sigma_{u0} \sigma_{d0} \sigma_{s0}) - 2G_V (n_u^2 + n_d^2 + n_s^2). \quad (8)$$

## 2.2. Beta Equilibrated Cold Quark Matter

In this section, we will consider the thermodynamic properties of stellar matter composed of deconfined  $u, d, s$  quarks and electrons staying in  $\beta$ -equilibrium. For such matter, the thermodynamic grand potential at zero temperature can be written in the following form:

$$\begin{aligned} \Omega_{QP} = & \frac{3}{\pi^2} \sum_{f=u,d,s} \left( \int_0^\Lambda dk k^2 \sqrt{k^2 + M_{f0}^2} - \int_{(\pi^2 n_f)^{1/3}}^\Lambda dk k^2 \sqrt{k^2 + M_f^2} \right) \\ & - \sum_{f=u,d,s} n_f \sqrt{(\pi^2 n_f)^{2/3} + M_f^2} + 2G_s (\sigma_u^2 + \sigma_d^2 + \sigma_s^2 - \sigma_{u0}^2 - \sigma_{d0}^2 - \sigma_{s0}^2) \\ & - 4K (\sigma_u \sigma_d \sigma_s - \sigma_{u0} \sigma_{d0} \sigma_{s0}) - 2G_V (n_u^2 + n_d^2 + n_s^2) \\ & + \frac{1}{\pi^2} \int_0^{(3\pi^2 n_e)^{1/3}} dk k^2 \sqrt{k^2 + m_e^2} - n_e \sqrt{(3\pi^2 n_e)^{2/3} + m_e^2}. \end{aligned} \quad (9)$$

Chemical potentials of quarks are expressed in terms of constituent mass  $M_f$  and number density  $n_f$  of a quark of flavor  $f$

$$\mu_f(n_f, M_f) = \sqrt{(\pi^2 n_f)^{2/3} + M_f^2} + 4G_V n_f, \quad (f = u, d, s). \quad (10)$$

The chemical potential of electrons is a function of electron number density

$$\mu_e(n_e) = \sqrt{(3\pi^2 n_e)^{2/3} + m_e^2} \quad (11)$$

The quark condensates  $\sigma_f$  are expressed in terms of constituent mass  $M_f$  and number density  $n_f$  of a quark of flavor  $f$  as follows:

$$\sigma_f = -\frac{3M_f}{\pi^2} \int_{(\pi^2 n_f)^{1/3}}^\Lambda dk \frac{k^2}{\sqrt{k^2 + M_f^2}}, \quad (f = u, d, s). \quad (12)$$

In that stage when the neutrinos, created in the stellar core, completely come out of the star, the conditions of beta equilibrium will have the form

$$\mu_d(n_d, M_d) = \mu_u(n_u, M_u) + \mu_e(n_e), \quad (13)$$

$$\mu_s(n_s, M_s) = \mu_d(n_d, M_d). \quad (14)$$

The charge neutrality condition is given by

$$\frac{2}{3}n_u - \frac{1}{3}n_d - \frac{1}{3}n_s - n_e = 0. \quad (15)$$

For the baryon number density, we have

$$n_B = \frac{1}{3}(n_u + n_d + n_s). \quad (16)$$

The system of Equations (6) and (13)–(16) for a given value of  $n_B$  is a closed system of seven equations, the numerical solution of which makes it possible to find the constituent quark masses  $M_u, M_d, M_s$  and the particle number densities  $n_u, n_d, n_s, n_e$ . Then, using Equations (10)–(12), one can calculate the chemical potentials  $\mu_u, \mu_d, \mu_s, \mu_e$  and quark condensates  $\sigma_u, \sigma_d, \sigma_s$ . Knowledge of these characteristics allows one to obtain the EOS of

the quark phase in a parametric form. The quark phase pressure  $P_{QP}$  is determined by the expression:

$$P_{QP} = -\Omega_{QP}. \quad (17)$$

The energy density is expressed in terms of the thermodynamic grand potential density  $\Omega_{QP}$  as

$$\varepsilon_{QP} = \Omega_{QP} + \sum_{f=u,d,s} \mu_f n_f + \mu_e n_e. \quad (18)$$

Using Equation (9) for the grand-potential density, the expression for the energy density can be represented in the form

$$\begin{aligned} \varepsilon_{QP} = & \frac{3}{\pi^2} \sum_{f=u,d,s} \left( \int_0^\Lambda dk k^2 \sqrt{k^2 + M_{f0}^2} - \int_0^\Lambda dk k^2 \sqrt{k^2 + M_f^2} \right) + 2G_s (\sigma_u^2 + \sigma_d^2 + \sigma_s^2) \\ & - 2G_s (\sigma_{u0}^2 + \sigma_{d0}^2 + \sigma_{s0}^2) - 4K (\sigma_u \sigma_d \sigma_s - \sigma_{u0} \sigma_{d0} \sigma_{s0}) + 2G_V (n_u^2 + n_d^2 + n_s^2) \\ & + \frac{1}{\pi^2} \int_0^{(3\pi^2 n_e)^{1/3}} dk k^2 \sqrt{k^2 + m_e^2}. \end{aligned} \quad (19)$$

### 2.3. Numerical Results

In this section, we present the numerical results obtained according to the scheme described in the previous section for electrically neutral quark matter in beta equilibrium. For the numerical calculation, we have used the parameters of the NJL model given in Ref. [39],  $m_u = m_d = 5.5$  MeV,  $m_s = 140.7$  MeV,  $\Lambda = 602.3$  MeV,  $G_s = 1.835/\Lambda^2$ ,  $K = 12.36/\Lambda^5$ . The coupling constant of the vector interaction  $G_V$  is a free parameter of the model. In this work, we performed calculations for several values  $G_V/G_s = 0; 0.2; 0.4; 0.6$ .

In Figure 1, we show the numerical results for the constituent quark masses  $M_u, M_d, M_s$  and the chemical potentials of particles as a function of the baryon number density  $n_B$  for several values of vector coupling  $G_V$ . Strange quarks can exist in the system if the condition  $\mu_d(n_B) \geq M_s(n_B)$  is satisfied. The minimum value of the baryon density at which strange quarks appear, or as it is commonly called, the threshold for the appearance of  $s$ -quarks, is determined by the equation  $\mu_d(n_B^{s-thr}) = M_s(n_B^{s-thr})$ . Note that this threshold density depends on the vector coupling constant  $G_V$ .

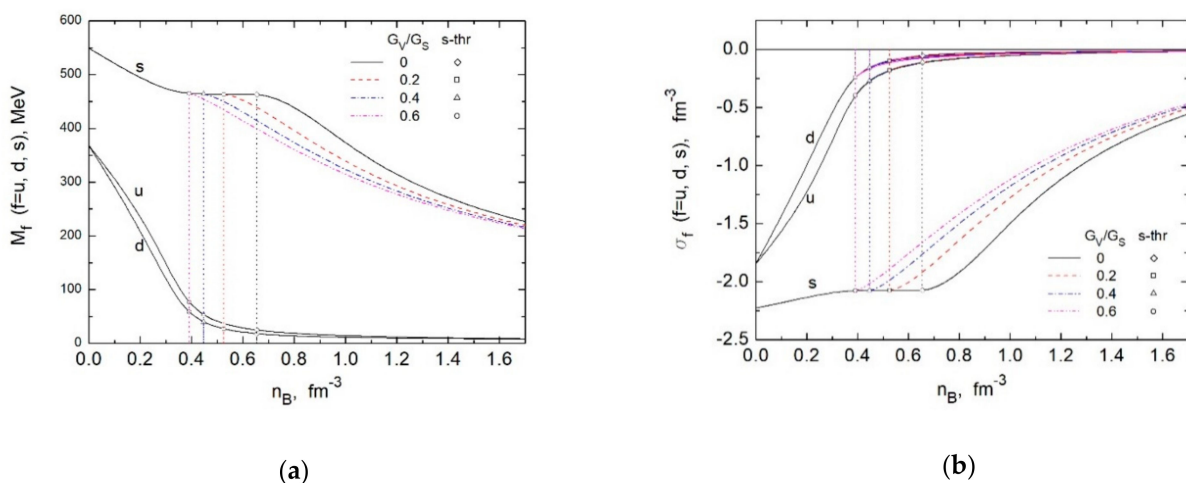


**Figure 1.** Baryon number density dependence of the constituent quark masses  $M_u(n_B), M_d(n_B), M_s(n_B)$  and quark condensates in electrically neutral beta equilibrium quark matter for several values of  $G_V/G_s$ . In (a), we show constituent quark masses as a function of baryon number density. In (b), we show the baryon number density dependence of quark condensates  $\sigma_u(n_B), \sigma_d(n_B), \sigma_s(n_B)$ . Vertical dotted lines show the threshold density for the appearance of strange quarks.

Note that in the NJL model considered here, the constituent quark masses depend on both the scalar coupling constant and the vector constant. The influence of the vector interaction on the constituent quark mass of a given flavor is carried out through quark condensates of all the flavors due to the mixing term in the gap, Equation (6). In contrast to this result, in the recent work [61], it was found that within the framework of the covariant spectator theory, the vector interaction completely determines the constituent quark mass, and any scalar (or pseudoscalar) interaction is completely decoupled due to chiral symmetry.

The parameters, such as strange-quark threshold  $n_B^{s-thr}$ , constituent quark masses  $M_u, M_d, M_s$ , baryonic chemical potential  $\mu_B$ , and energy per baryon  $E/A$  at threshold density in electrically neutral beta equilibrium quark matter for  $G_V/G_s = 0; 0.2; 0.4; 0.6$  are presented in Table 1. As can be seen from Figure 1 and Table 1, the larger the vector coupling constant  $G_V$ , the lower the threshold density  $n_B^{s-thr}$  for the appearance of  $s$ -quarks. In addition, the constituent  $u$  and  $d$  quark masses are dependent on the vector coupling very weakly. The dependences of the constituent  $s$ -quark mass and corresponding condensate  $\sigma_s$  on vector coupling are weaker in the region of densities below the threshold  $n_B^{s-thr}$ , and are more significant in the region above that threshold.

**Table 1.** Constituent masses, baryonic chemical potential, and energy per baryon in deconfined quark matter at strange quark threshold density  $n_B^{s-thr}$  for various values of vector coupling  $G_V$ .

$G_V/G_s$	$n_B^{s-thr} \text{ fm}^{-3}$	$M_u \text{ MeV}$	$M_d \text{ MeV}$	$M_s \text{ MeV}$	$\mu_B \text{ MeV}$	$E/A \text{ MeV}$
0	0.6545	24.87	17.98	462.94	1294.9	1142.55
0.2	0.5259	36.887	27.1544	463.241	1287.63	1156.71
0.4	0.4464	53.4407	40.0216	463.916	1285.07	1174.3
0.6	0.3901	76.7248	58.6001	465.397	1287.8	1192.72

The dependence of the strange quarks appearance threshold density  $n_B^{s-thr}$  on the value of the vector coupling constant  $G_V$  is displayed in Figure 2. It can be seen that the larger the vector coupling constant, the lower the threshold for the appearance of strange quarks in quark matter. On the  $(n_B^{s-thr}, G_V)$  plane of Figure 2, the region below the curve corresponds to the  $ude$  composition of matter, and the region above the curve corresponds to the  $udse$  composition.

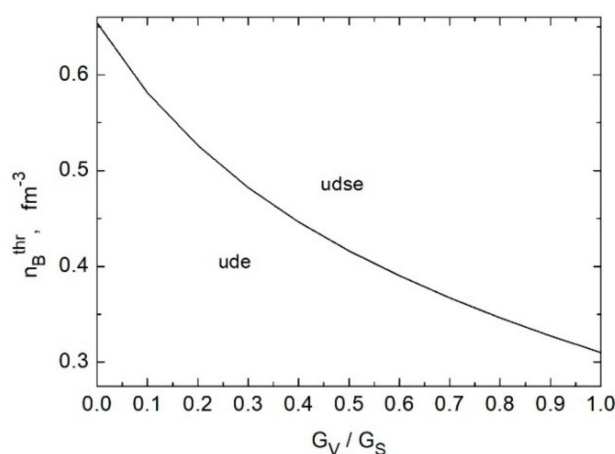


**Figure 2.** Threshold density for the appearance of strange quarks as a function of vector coupling constant  $G_V$ .

Figure 3 shows the results of the numerical solution of the gap equations, where (a) and (b) present the constituent-quark masses  $M_u, M_d, M_s$  and the pressure of the quark matter  $P$ , respectively, as functions of the baryon chemical potential  $\mu_B$  for different values of the vector coupling constant  $G_V$ . As can be seen from this figure, for a sufficiently small value

of the vector coupling constant  $G_V$ , the functions of the mass dependence on the baryonic chemical potential have regions of ambiguity. This ambiguity leads to a phase transition in nonstrange quark matter with an abrupt change in the baryon number density (see the inset in Figure 3b). In this case, nonstrange quark matter will have the instability region. With a sufficiently large value of the coupling constant  $G_V$ , this ambiguity disappears.

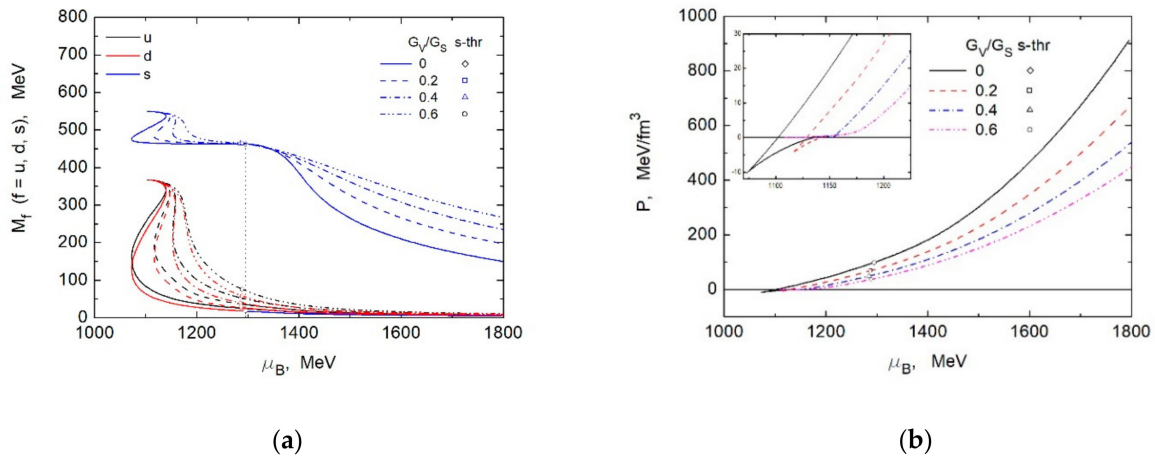


**Figure 3.** Constituent-quark masses  $M_u, M_d, M_s$  (a) and pressure  $P$  (b) as functions of baryon chemical potential  $\mu_B$ . Vertical dotted line in (a) denotes the strange quark threshold in the case of  $G_V = 0$ . The inset in (b) shows a zoomed view of the region of the lower boundary.

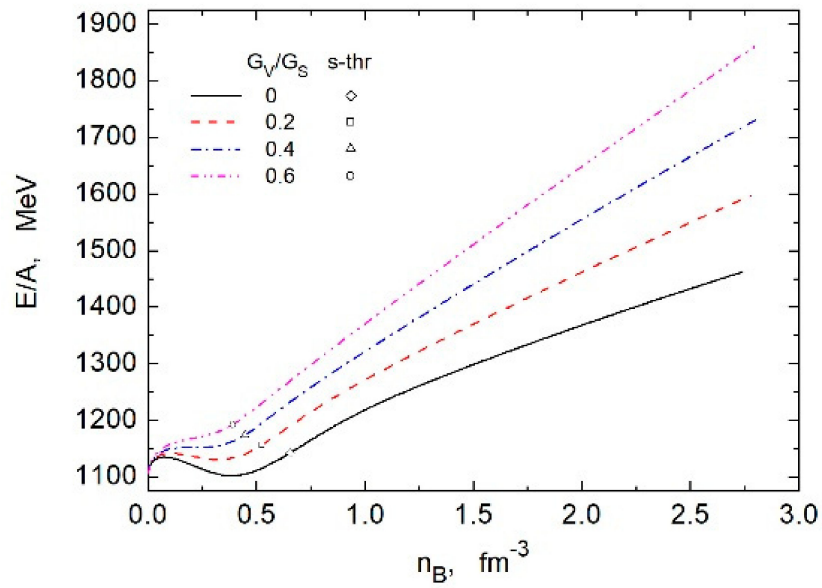
It is known that at a given value of the pressure, the greater the chemical potential, the greater the stiffness of the EOS. Figure 3b shows that the inclusion of the vector interaction term leads to an increase in the stiffness of the EOS.

In Figure 4, we show the energy per baryon  $E/A = \varepsilon/n_B$  as a function of the baryon number density  $n_B$  for different values of the vector coupling constant  $G_V$ . It is seen that the greater the vector coupling constant, the greater the energy per baryon. Note that the value of energy per baryon in beta equilibrium quark matter exceeds the similar value in the most bound nucleus ( $M_{56Fe}/56 = 930.4$  MeV). This means that the hypothesis on the absolute stability of strange quark matter [31–34] within the framework of the NJL model is not realized. In the considered version of the NJL model, the three-flavor quark matter in beta equilibrium at pressures below a certain critical value will be unstable with respect to the transition to matter with a hadronic structure. Compact stars, in which the central pressure is greater than this critical value, are hybrid stars.

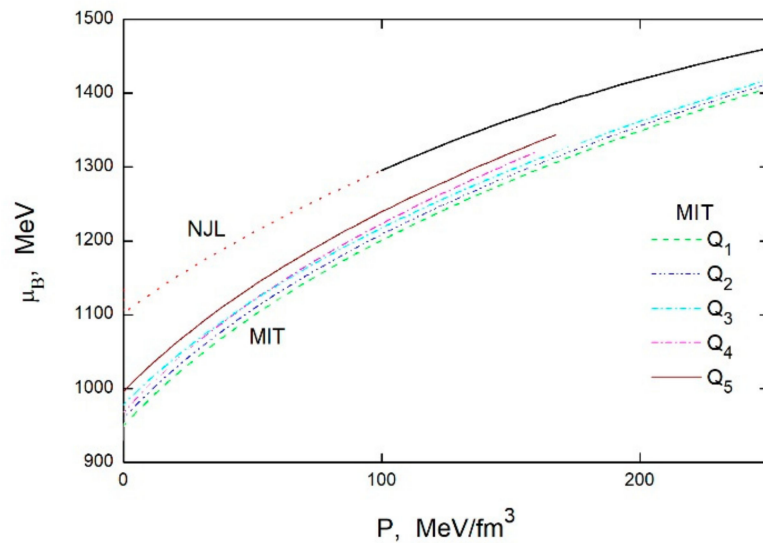
It should be noted that, in the MIT bag model, at comparatively small values of the bag parameter  $B$ , the energy per baryon in the three-flavor quark matter at zero pressure can be less than 930.4 MeV. In this case, the three-flavor quark matter will be absolutely stable; therefore, so-called strange stars will exist.

Figure 5 compares the results of our calculations in the framework of the NJL model without inclusion of the vector interaction term ( $G_V = 0$ ) with the corresponding results obtained in Ref. [14] in the extended MIT bag model, in which the interaction between quarks is taken into account in the one-gluon exchange approximation. The calculations in the MIT bag model were performed for five different sets of values of strange quark mass  $m_s$ , bag parameter  $B$ , and strong interaction constant  $\alpha_c$ , as is shown in Table 2.

As we can see in Figure 5, at a given pressure, the chemical potential in the NJL model is greater than that in the MIT model. The discrepancy between these values becomes even stronger when the vector interaction is taken into account. This kind of difference in the relationship between the baryon chemical potential and pressure leads to a greater value of the coexistence pressure  $P_0^{NJL}$  of the two phases in the NJL model compared with the coexistence pressure  $P_0^{MIT}$  in the MIT model.



**Figure 4.** Energy per baryon as a function of the baryon number density for different values of the vector coupling constant  $G_V$ . Symbols, such as diamond, square, triangle, and circle, denote the strange-quark formation thresholds for  $G_V/G_S = 0; 0.2; 0.4; 0.6$ , respectively.



**Figure 5.** Baryon chemical potential as a function of the pressure for electrically neutral quark matter in beta-equilibrium. Comparison between the results in the Nambu–Jona-Lasinio (NJL) model at  $G_V = 0$  and the MIT bag model at various values of the bag parameters is shown in Table 2.

**Table 2.** MIT bag model parameters shown in Figure 5 for comparing with our results obtained within the NJL model.

MIT	$Q_1$	$Q_2$	$Q_3$	$Q_4$	$Q_5$
$m_s$ , MeV	175	175	175	200	200
$B$ , MeV/fm <sup>3</sup>	55	55	60	55	60
$\alpha_c$	0.5	0.6	0.6	0.5	0.6

### 3. Hadronic Matter Phase

Relativistic mean field (RMF) theory [62–64] is used to describe the hadronic matter phase. In the RMF approach of quantum hydrodynamics (QHD), it is believed that hadrons interact through the exchange of various mesons. In this work, we assumed that the beta equilibrium hadronic matter consists of protons ( $p$ ), neutrons ( $n$ ), and electrons ( $e$ ), and that the exchange particles are: Isoscalar-scalar meson  $\sigma$ ; isoscalar-vector meson  $\omega$ ; isovector-scalar meson  $\delta$ ; isovector-vector meson  $\rho$ .

The relativistic nonlinear Lagrangian density for hadronic matter consisting of protons, neutrons, and electrons reads

$$\begin{aligned} \mathcal{L}_{RMF} = & \bar{\psi}_N \left[ \gamma^\mu \left( i\partial_\mu - g_\omega \omega_\mu(x) - \frac{1}{2} g_\rho \vec{\tau}_N \cdot \vec{\rho}_\mu(x) \right) - \left( m_N - g_\sigma \sigma(x) - g_\delta \vec{\tau}_N \cdot \vec{\delta}(x) \right) \right] \psi_N \\ & + \frac{1}{2} \left( \partial_\mu \sigma(x) \partial^\mu \sigma(x) - m_\sigma^2 \sigma(x)^2 \right) - \frac{b}{3} m_N (g_\sigma \sigma(x))^3 - \frac{c}{4} (g_\sigma \sigma(x))^4 \\ & + \frac{1}{2} m_\omega^2 \omega^\mu(x) \omega_\mu(x) - \frac{1}{4} \Omega_{\mu\nu}(x) \Omega^{\mu\nu}(x) + \frac{1}{2} \left( \partial_\mu \vec{\delta}(x) \partial^\mu \vec{\delta}(x) - m_\delta^2 \vec{\delta}(x)^2 \right) \\ & + \frac{1}{2} m_\rho^2 \vec{\rho}^\mu(x) \vec{\rho}_\mu(x) - \frac{1}{4} \mathfrak{R}_{\mu\nu}(x) \mathfrak{R}^{\mu\nu}(x) + \bar{\psi}_e (i\gamma^\mu \partial_\mu - m_e) \psi_e, \end{aligned} \quad (20)$$

where  $\psi_N = \begin{pmatrix} \psi_p \\ \psi_n \end{pmatrix}$  is the isospin doublet of nucleon bispinors,  $\vec{\tau}_N$  are  $2 \times 2$  Pauli isospin matrices,  $\sigma(x)$ ,  $\omega_\mu(x)$ ,  $\vec{\delta}(x)$ ,  $\vec{\rho}_\mu(x)$  are exchange meson fields at space-time point  $x = x_\mu = (t, x, y, z)$ ,  $m_N$ ,  $m_e$ ,  $m_\sigma$ ,  $m_\omega$ ,  $m_\delta$ ,  $m_\rho$  are the masses of the free particles, and  $\Omega_{\mu\nu}(x)$  and  $\mathfrak{R}_{\mu\nu}(x)$  are antisymmetric tensors of the vector fields  $\omega_\mu(x)$  and  $\vec{\rho}_\mu(x)$ , respectively.

In the mean-field approximation, the meson quantum fields are replaced by their expectation values. The energy density and pressure of the hadronic matter phase in the RMF approach are written by (for details, see Ref. [57])

$$\begin{aligned} \varepsilon_{HP} = & \frac{1}{\pi^2} \int_0^{k_F(n_B)(1-\alpha)^{1/3}} dk k^2 \sqrt{k^2 + (m_N - \sigma - \delta)^2} + \frac{b}{3} m_N \sigma^3 + \frac{c}{4} \sigma^4 \\ & + \frac{1}{\pi^2} \int_0^{k_F(n_B)(1+\alpha)^{1/3}} dk k^2 \sqrt{k^2 + (m_N - \sigma + \delta)^2} + \frac{1}{2} \left( \frac{\sigma^2}{a_\sigma} + \frac{\omega^2}{a_\omega} + \frac{\delta^2}{a_\delta} + \frac{\rho^2}{a_\rho} \right) \\ & + \frac{1}{\pi^2} \int_0^{\sqrt{\mu_e^2 - m_e^2}} dk k^2 \sqrt{k^2 + m_e^2}, \end{aligned} \quad (21)$$

$$\begin{aligned} P_{HP} = & \frac{1}{\pi^2} \int_0^{k_F(n_B)(1-\alpha)^{1/3}} dk k^2 \left( \sqrt{k_F(n_B)^2 (1-\alpha)^{2/3} + (m_N - \sigma - \delta)^2} - \sqrt{k^2 + (m_N - \sigma - \delta)^2} \right) \\ & + \frac{1}{\pi^2} \int_0^{k_F(n_B)(1+\alpha)^{1/3}} dk k^2 \left( \sqrt{k_F(n_B)^2 (1+\alpha)^{2/3} + (m_N - \sigma + \delta)^2} - \sqrt{k^2 + (m_N - \sigma + \delta)^2} \right) \\ & - \frac{b}{3} m_N \sigma^3 - \frac{c}{4} \sigma^4 + \frac{1}{2} \left( -\frac{\sigma^2}{a_\sigma} + \frac{\omega^2}{a_\omega} - \frac{\delta^2}{a_\delta} + \frac{\rho^2}{a_\rho} \right) - \frac{1}{\pi^2} \int_0^{\sqrt{\mu_e^2 - m_e^2}} dk k^2 \sqrt{k^2 + m_e^2} \\ & + \frac{1}{3\pi^2} \mu_e (\mu_e^2 - m_e^2)^{3/2}, \end{aligned} \quad (22)$$

where  $n_B$  notes the baryon number density of the hadronic matter phase,  $\alpha = (n_n - n_p)/n_B$  is the asymmetry parameter,  $\mu_e$  is the electron chemical potential, and  $k_F(n_B) = (3\pi^2 n_B/2)^{1/3}$ . The renamed meson mean-fields are expressed in terms of nonvanishing expectation values of corresponding meson fields as follows:

$$\sigma \equiv g_\sigma \langle \sigma(x) \rangle, \quad \omega \equiv g_\omega \langle \omega_0(x) \rangle, \quad \delta \equiv g_\delta \langle \delta^{(3)}(x) \rangle, \quad \rho \equiv g_\rho \langle \rho_0^{(3)}(x) \rangle. \quad (23)$$

Parameters  $a_\sigma$ ,  $a_\omega$ ,  $a_\delta$ , and  $a_\rho$  are expressed in terms of the corresponding meson–nucleon coupling constant and meson mass, as follows:

$$a_\sigma = (g_\sigma/m_\sigma)^2, \quad a_\omega = (g_\omega/m_\omega)^2, \quad a_\delta = (g_\delta/m_\delta)^2, \quad a_\rho = (g_\rho/m_\rho)^2. \quad (24)$$

The equations for the meson mean-fields in homogeneous hadronic matter can be written in the form

$$\sigma = a_\sigma \left( n_{sp}(n_B, \alpha) + n_{sn}(n_B, \alpha) - b m_N \sigma^2 - c \sigma^3 \right), \quad (25)$$

$$\omega = a_\omega n_B, \quad (26)$$

$$\delta = a_\delta \left( n_{sp}(n_B, \alpha) - n_{sn}(n_B, \alpha) \right), \quad (27)$$

$$\rho = -\frac{1}{2} a_\rho n_B \alpha, \quad (28)$$

where  $n_{sp}(n_B, \alpha)$  and  $n_{sn}(n_B, \alpha)$  are the scalar densities of protons and neutrons, respectively, which are written in the form

$$n_{sp}(n_B, \alpha) = \frac{1}{\pi^2} \int_0^{k_F(n_B)(1-\alpha)^{1/3}} dk k^2 \frac{m_N - \sigma - \delta}{\sqrt{k^2 + (m_N - \sigma - \delta)^2}}, \quad (29)$$

$$n_{sn}(n_B, \alpha) = \frac{1}{\pi^2} \int_0^{k_F(n_B)(1+\alpha)^{1/3}} dk k^2 \frac{m_N - \sigma + \delta}{\sqrt{k^2 + (m_N - \sigma + \delta)^2}}. \quad (30)$$

The chemical potentials of nucleons are given by

$$\begin{aligned} \mu_p(n_B, \alpha) &= \sqrt{k_F(n_B)^2 (1-\alpha)^{2/3} + (m_N - \sigma - \delta)^2} + \omega + \frac{1}{2}\rho, \\ \mu_n(n_B, \alpha) &= \sqrt{k_F(n_B)^2 (1+\alpha)^{2/3} + (m_N - \sigma + \delta)^2} + \omega - \frac{1}{2}\rho, \end{aligned} \quad (31)$$

Taking into account the electrical neutrality condition,  $n_e = n_B(1-\alpha)/2$ , the electron chemical potential can be expressed in terms of the baryon density and the asymmetry parameter

$$\mu_e(n_B, \alpha) = \sqrt{\left( \frac{3}{2} \pi^2 n_B (1-\alpha) \right)^{2/3} + m_e^2} \quad (32)$$

For neutron star matter consisting of protons, neutrons, and electrons, the  $\beta$ -equilibrium condition without trapped neutrinos is given by

$$\mu_n = \mu_p + \mu_e. \quad (33)$$

In the present calculation, we use the parameter set given in Ref. [65] and listed in Table 3.

**Table 3.** The relativistic mean field (RMF) parameter set used in this work for calculations.

$a_\sigma \text{ fm}^2$	$a_\omega \text{ fm}^2$	$a_\delta \text{ fm}^2$	$a_\rho \text{ fm}^2$	$b \text{ fm}^{-1}$	$c$
9.154	4.828	2.5	13.621	$1.654 \cdot 10^{-2}$	$1.319 \cdot 10^{-2}$

The system of Equations (25)–(28) and (33) for a given value of baryon number density  $n_B$  is a closed set of equations, the numerical solution of which makes it possible to find the meson mean-fields  $\sigma$ ,  $\omega$ ,  $\delta$ ,  $\rho$  and asymmetry parameter  $\alpha$ . Knowledge of these characteristics as functions of baryon number density makes it possible to obtain a parametric form of the EOS of hadronic matter presented in (21) and (22).

#### 4. Compact Star Matter EOS with Hadron–Quark Phase Transition

To construct a hybrid EOS for compact-star matter, it is necessary, in addition to the EOS of the quark phase and hadron phase separately, to also have the type of phase transition. The phase transition from hadronic matter to quark matter is principally different from the phase transition of ordinary matter consisting of atoms. In the case of ordinary atomic matter, there is only one conserved quantity, the number of atoms. In the case of a phase transition from hadronic matter to quark matter, there are two conserved quantities, the baryon number and the electric charge. Depending on the value of surface tension between hadronic matter and quark matter, one of the two scenarios of a phase transition can take place.

If the surface tension coefficient is less than a certain critical value, then the phase transition occurs with the formation of a mixed phase (Gibbs scenario). In the mixed phase, the condition of global charge neutrality is satisfied. Anyway, both the hadron phase and the quark phase are allowed to be separately charged [66]. In the Gibbs (Glendenning) construction scenario, the interface between the two phases is smooth and the dependence of the energy density on pressure is a continuous function.

Otherwise, when the value of the surface tension coefficient is greater than this critical value, the phase transition is an ordinary first-order phase transition. In this case, the condition of charge neutrality is satisfied for each phase, separately. Such a phase transition occurs at a certain constant pressure value, and the characteristics of the phase transition are determined by the Maxwell construction (Maxwell scenario). The pressure dependence of the energy density is a discontinuous function with a jump at the transition pressure.

As the value of the surface tension coefficient between quark matter and hadronic matter is still quite uncertain, it is impossible to determine which of the above two scenarios actually takes place. In this work, we assume that the surface tension between quark matter and hadronic matter is so strong that the phase transition occurs according to the Maxwell scenario.

Characteristics of the phase transition are determined according to the requirement for the simultaneous fulfillment of the conditions of mechanical and chemical equilibrium

$$P_{HP} = P_{QP} = P_0, \quad \mu_B^{HP} = \mu_B^{QP} = \mu_{B0}, \quad (34)$$

where  $\mu_B^{HP} = \mu_n$  and  $\mu_B^{QP} = \mu_u + \mu_d + \mu_s$  are the baryon chemical potentials for hadronic and quark phases, respectively.

The numerical solution of Equation (33) makes it possible to obtain the values of the transition pressure  $P_0$  and the baryon chemical potential  $\mu_{B0}$  at the phase transition. Knowledge of these quantities will allow the calculation of the remaining characteristics of the phase transition, such as: Particle number densities  $n_{H0}$ ,  $n_{Q0}$  and the energy densities  $\varepsilon_{H0}$ ,  $\varepsilon_{Q0}$  for hadronic and quark phases, respectively. Graphically, these parameters can be determined by constructing a common tangent to the curves  $\varepsilon_{HP}(n_B)$  and  $\varepsilon_{QP}(n_B)$ . The phase transition parameters can also be found by intersection of the curves  $P_{HP}(\mu_B)$  and  $P_{QP}(\mu_B)$  corresponding to the hadronic and quark phases.

An important parameter for a first-order phase transition is the quantity

$$\lambda = \frac{\varepsilon_{Q0}}{\varepsilon_{H0} + P_0}. \quad (35)$$

The value of this parameter is decisive from the point of view of stability of the infinitesimal core of the dense phase formed in the center of the neutron star [67]. If  $\lambda < 3/2$ , then the infinitesimal quark matter core inside a neutron star is stable. The mass of the star as a function of the central pressure, at the value of the central pressure  $P_c = P_0$ , has a break, while maintaining a monotonically increasing character near this point. If the condition  $\lambda > 3/2$  is satisfied, the mass of the star at the central pressure  $P_c = P_0$  has a local maximum, which means that the infinitesimal core of quark matter newly formed in the center of the star is unstable. During accretion of matter onto a star, when the central

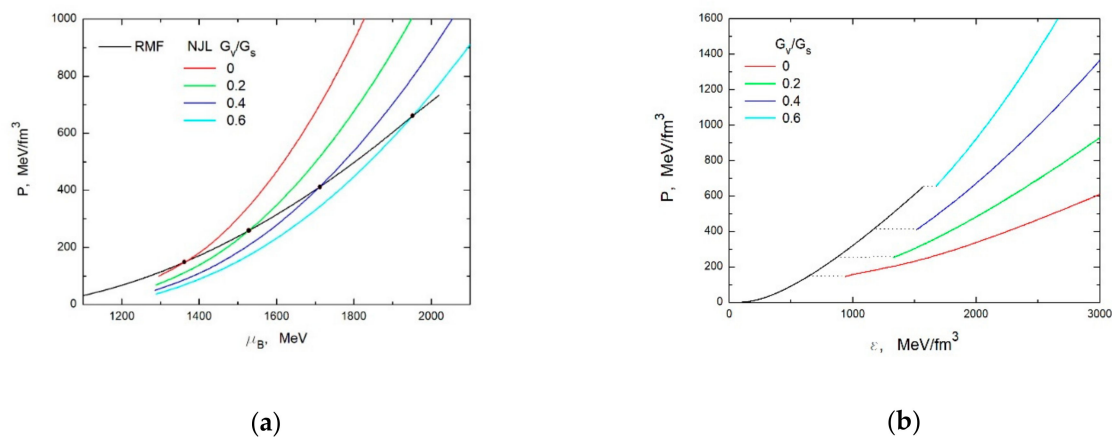
pressure reaches the value  $P_0$ , a core of finite size consisting of quark matter will be abruptly formed in the center.

Table 4 shows the phase transition characteristics for different values of vector coupling constant  $G_V$ . Note that within the framework of the model considered here, the value of the jump parameter  $\lambda$  with and without inclusion of the vector interaction term always remains less than  $3/2$ .

**Table 4.** First-order phase transition parameters for different ratios of vector and scalar coupling constants.

$G_V/G_s$	$P_0$ MeV/fm <sup>3</sup>	$\varepsilon_{H0}$ MeV/fm <sup>3</sup>	$n_{H0}$ fm <sup>-3</sup>	$\varepsilon_{Q0}$ MeV/fm <sup>3</sup>	$n_{Q0}$ fm <sup>-3</sup>	$\mu_{B0}$ MeV	$\lambda$
0	150.2	646.88	0.5841	958.56	0.8128	1364.4	1.20
0.2	258.5	879.39	0.7449	1347.69	1.1343	1527.6	1.18
0.4	409.9	1163.47	0.9205	1515.03	1.3189	1709.4	0.96
0.6	659.5	1582.41	1.1495	1680.02	1.5420	1950.8	0.75

In Figure 6a, we show the pressure  $P$  as a function of baryonic chemical potential  $\mu_B$  for both the hadronic matter within the RMF model and the deconfined quark matter within the NJL model. In the case of the Maxwell's construction, the phase transition is identified by the crossing points between the curves corresponding to the hadronic and quark phases in the  $P - \mu_B$  plane. In Figure 6b, we plot the EOS of hybrid star matter with a sharp (constant pressure) quark–hadron phase transition for different ratios of vector and scalar coupling constants:  $G_V/G_s = 0, 0.2, 0.4, 0.6$ . From this figure, one can find that the greater the vector coupling constant  $G_V$ , the greater the stiffness of the EOS for quark matter, and the greater the phase transition pressure  $P_0$ .



**Figure 6.** (a) Pressure as a function of baryonic chemical potential for the hadronic matter within the RMF model and for the deconfined quark matter within the NJL model. (b) Equation of state (EOS) of hybrid star matter with deconfinement phase transition for different ratios of vector and scalar coupling constants  $G_V/G_s$ .

## 5. Discussion and Conclusions

In this work, we have studied the phase transition from hadronic matter to quark matter, and have built the hybrid EOSs for the compact-star matter by using the Maxwell construction. In order to describe the thermodynamic properties of hadronic matter, an improved RMF theory was applied, in which, in addition to the fields of  $\sigma$ ,  $\omega$  and  $\rho$  mesons, the effective field of the scalar-isovector  $\delta$ -meson was also taken into account.

The thermodynamic properties of quark matter are studied in the framework of the SU (3) local NJL model, in which the vector interactions were also taken into account. For different values of the vector coupling constant  $G_V$  the gap equations for the constituent quark masses were numerically solved, and the thermodynamic characteristics of  $\beta$ -equilibrium charge neutral quark matter were found. The threshold values of the

baryon number density, corresponding to the appearance of a strange quark, have been determined. It is shown that the greater the value of the vector coupling constant  $G_V$ , the lower the threshold density  $n_B^{s-thr}$  of the appearance of  $s$ -quarks.

The influence of vector interactions on constituent quark masses and quark condensates was investigated. It is shown that the constituent masses of  $u$  and  $d$  quarks, and the condensates of these quarks,  $\langle \bar{\psi}_u \psi_u \rangle$ ,  $\langle \bar{\psi}_d \psi_d \rangle$  weakly depend on the value of the vector coupling constant  $G_V$ . The dependence of the  $s$ -quark constituent mass and the corresponding condensate  $\langle \bar{\psi}_s \psi_s \rangle$  on the vector coupling constant  $G_V$  is weaker in the region below the threshold for the appearance of the  $s$ -quark, and is more significant in the region above the threshold. The larger the vector coupling constant, the lower the constituent  $s$ -quark mass in the density region above the  $s$ -quark threshold.

By investigating the dependence of constituent quark masses on the baryon number density, we found that for sufficiently small values of the vector coupling constant in the region below the  $s$ -quark threshold, the functions  $M_f(\mu_B)$  ( $f = u, d, s$ ) have an ambiguity region. This ambiguity leads to a phase transition in nonstrange quark matter with an abrupt change in the baryon number density. In this case, the nonstrange quark matter will get an instability region. With a sufficiently large value of the coupling constant  $G_V$ , this ambiguity disappears.

We also studied the energy per baryon for  $\beta$ -equilibrium and charge neutral quark matter, and found that it exceeds the similar value in the most bound nucleus,  $M_{56Fe}/56 = 930.4$  MeV. This means that the Bodmer-Witten-Terazawa-Itoh hypothesis about the absolute stability of the strange quark matter in the framework of the NJL model is not realized.

Comparison of the results of the NJL model with similar results of the MIT bag model showed that, at a given pressure, the baryon chemical potential in the NJL model is greater than in the MIT bag model. This kind of difference leads to a greater value of the coexistence pressure for the two phases  $P_0^{NJL}$  in the NJL model compared with the coexistence pressure  $P_0^{MIT}$  in the MIT bag model. It is shown that the greater the vector coupling constant,  $G_V$ , the greater the stiffness of the EOS for quark matter, and the greater the phase transition pressure  $P_0$ .

We have also calculated the density jump parameter,  $\lambda = \varepsilon_{Q0}/(\varepsilon_{H0} + P_0)$  which is important from the point of view of stability of the infinitesimal core of the deconfined quark matter formed in the center of a compact star. In the model, considered in this paper, the jump parameter  $\lambda < 3/2$  satisfies the stability condition for the infinitesimal core of the quark phase.

The hybrid equations of state, obtained in this work for different values of the vector coupling constant, will make it possible to calculate the integral and structural characteristics of hybrid quark–hadron stars, also to study the influence of the vector coupling constant on the properties of the star. A separate article will be devoted to these problems in the future.

**Funding:** This work was done in the Research Laboratory of Superdense Star Physics at Yerevan State University and is supported by the Science Committee of the Ministry of Education, Science, Culture, and Sports of the Republic of Armenia.

**Conflicts of Interest:** The author declares no conflict of interest.

## References

1. Glendenning, N.K. *Compact Stars: Nuclear Physics, Particle Physics, and General Relativity*, 2nd ed.; Appenzeller, I., Börner, G., Harwit, M., Kippenhahn, R., Lequeux, J., Stritmatter, P.A., Trimble, V., Eds.; Springer: Berlin/Heidelberg, Germany, 2000.
2. Haensel, P.; Potekhin, A.Y.; Yakovlev, D.G. *Neutron Stars 1: Equation of State and Structure*; Kluwer Academic Publishers Boston: London, UK, 2007.
3. Lattimer, J.M.; Prakash, M. The physics of neutron stars. *Science* **2004**, *304*, 536–542. [[CrossRef](#)] [[PubMed](#)]
4. Weber, F.; Negreiros, R.; Rosenfield, P.; Stejner, M. Pulsars as astrophysical laboratories for nuclear and particle physics. *Prog. Part. Nucl. Phys.* **2007**, *59*, 94–113. [[CrossRef](#)]
5. De Carvalho, S.M.; Negreiros, R.; Orsaria, M.; Contrera, G.A.; Weber, F.; Spinella, W. Thermal evolution of hybrid stars within the framework of a nonlocal Nambu–Jona-Lasinio model. *Phys. Rev. C* **2015**, *92*, 035810. [[CrossRef](#)]

6. Grigorian, H.; Blaschke, D.; Voskresensky, D.N. Cooling of neutron stars and hybrid stars with a stiff hadronic EoS. *Phys. Part. Nuclei* **2015**, *46*, 849–853. [[CrossRef](#)]
7. Alaverdyan, A.G.; Alaverdyan, G.B.; Melikyan, S.R. Energy release associated with quark phase transition in neutron stars: Comparative analysis of Maxwell and Glendenning scenarios. *Int. J. Mod. Phys. CS* **2012**, *18*, 1–9. [[CrossRef](#)]
8. Demorest, P.B.; Pennucci, T.; Ransom, S.M.; Roberts, M.S.E.; Hessels, J.W.T. A two-solar-mass neutron star measured using Shapiro delay. *Nature* **2010**, *467*, 1081–1083. [[CrossRef](#)] [[PubMed](#)]
9. Antoniadis, J.; Freire, P.C.C.; Wex, N.; Tauris, T.M.; Lynch, R.S.; van Kerkwijk, M.H.; Kramer, M.; Bassa, C.; Dhillon, V.S.; Driebe, T.; et al. A massive pulsar in a compact relativistic binary. *Science* **2013**, *340*, 1233232. [[CrossRef](#)]
10. Chodos, A.; Jaffe, R.L.; Johnson, K.; Thorn, C.B.; Weisskopf, V.F. New extended model of hadrons. *Phys. Rev. D* **1974**, *9*, 3471–3495. [[CrossRef](#)]
11. Schertler, K.; Greiner, C.; Schaffner-Bielich, J.; Thoma, M.H. Quark phases in neutron stars and a third family of compact stars as signature for phase transitions. *Nucl. Phys. A* **2000**, *677*, 463–490. [[CrossRef](#)]
12. Alaverdyan, G.B.; Harutyunyan, A.R.; Vartanyan, Y.L. Low-mass quark stars or quark white dwarfs. *Astrophysics* **2001**, *44*, 265–275. [[CrossRef](#)]
13. Burgio, G.F.; Baldo, M.; Sahu, P.K.; Schulze, H.-J. Hadron-quark phase transition in dense matter and neutron stars. *Phys. Rev. C* **2002**, *66*, 025802. [[CrossRef](#)]
14. Alaverdyan, G.B.; Harutyunyan, A.R.; Vartanyan, Y.L. Neutron stars with a quark core. I. equations of state. *Astrophysics* **2003**, *46*, 361–367. [[CrossRef](#)]
15. Alaverdyan, G.B.; Harutyunyan, A.R.; Vartanyan, Y.L. Neutron stars with a quark core. II. basic integral and structural parameters. *Astrophysics* **2004**, *47*, 52–64. [[CrossRef](#)]
16. Nicotra, O.E.; Baldo, M.; Burgio, G.F.; Schulze, H.-J. Hybrid protoneutron stars with the MIT bag model. *Phys. Rev. D* **2006**, *74*, 123001. [[CrossRef](#)]
17. Sharma, B.K.; Panda, P.K.; Patra, S.K. Phase transition and properties of a compact star. *Phys. Rev. C* **2007**, *75*, 035808. [[CrossRef](#)]
18. Alaverdyan, G.B. Scalar-isovector  $\delta$ -meson in the relativistic mean field theory and the structure of neutron stars with a quark core. *Gravit. Cosmol.* **2009**, *15*, 5–9. [[CrossRef](#)]
19. Alaverdyan, G.B. Influence of a Scalar-isovector  $\delta$ -meson field on the quark phase structure in neutron stars. *Res. Astron. Astrophys.* **2010**, *10*, 1255–1264. [[CrossRef](#)]
20. Negreiros, R.; Dexheimer, V.A.; Schramm, S. Quark core impact on hybrid star cooling. *Phys. Rev. C* **2012**, *85*, 035805. [[CrossRef](#)]
21. Alaverdyan, G.B.; Vartanyan, Y.L. Maximum mass of hybrid stars in the quark bag model. *Astrophysics* **2017**, *60*, 563–571. [[CrossRef](#)]
22. Khanmohamadi, S.; Moshfegh, H.R.; Atashbar Tehrani, S. Hybrid star within the framework of a lowest-order constraint variational method. *Phys. Rev. D* **2020**, *101*, 023004. [[CrossRef](#)]
23. Alcock, C.; Farhi, E.; Olinto, A. Strange stars. *Astrophys. J.* **1986**, *310*, 261–272. [[CrossRef](#)]
24. Hajyan, G.S.; Vartanyan, Y.L.; Grigoryan, A.K. Strange stars and their cooling with positron electrical neutralization of quark matter. *Astrophysics* **1999**, *42*, 467–476. [[CrossRef](#)]
25. Jaikumar, P.; Reddy, S.; Steiner, A.W. Strange star surface: A crust with nuggets. *Phys. Rev. Lett.* **2006**, *96*, 041101. [[CrossRef](#)] [[PubMed](#)]
26. Alford, M.G.; Rajagopal, K.; Reddy, S.; Steiner, A.W. Stability of strange star crusts and strangelets. *Phys. Rev. D* **2006**, *73*, 114016. [[CrossRef](#)]
27. Vartanyan, Y.L.; Hajyan, G.S.; Grigoryan, A.K.; Sarkisyan, T.R. Stability of strange dwarfs I: Static criterion for stability. Statement of the problem. *Astrophysics* **2009**, *52*, 300–306. [[CrossRef](#)]
28. Alford, M.G.; Han, S.; Prakash, M. Generic conditions for stable hybrid stars. *Phys. Rev. D* **2013**, *88*, 083013. [[CrossRef](#)]
29. Hajyan, G.S.; Vartanyan, Y.L. Is EG 50 a white or strange dwarf? *Astrophysics* **2017**, *60*, 553–562. [[CrossRef](#)]
30. Vásquez Flores, C.; Lugones, G. Constraining color flavor locked strange stars in the gravitational wave era. *Phys. Rev. C* **2017**, *95*, 025808. [[CrossRef](#)]
31. Itoh, N. Hydrostatic equilibrium of hypothetical quark stars. *Prog. Theor. Phys.* **1970**, *44*, 291–292. [[CrossRef](#)]
32. Bodmer, A.R. Collapsed nuclei. *Phys. Rev. D* **1971**, *4*, 1601–1606. [[CrossRef](#)]
33. Terazawa, H. INS-Report-336, University of Tokyo, 1979; Super-hypernuclei in the quark-shell model. *J. Phys. Soc. Jpn.* **1989**, *58*, 3555–3563. [[CrossRef](#)]
34. Witten, E. Cosmic separation of phases. *Phys. Rev. D* **1984**, *30*, 272–285. [[CrossRef](#)]
35. Nambu, Y.; Jona-Lasinio, G. Dynamical model of elementary particles based on an analogy with superconductivity. I. *Phys. Rev.* **1961**, *122*, 345–358. [[CrossRef](#)]
36. Nambu, Y.; Jona-Lasinio, G. Dynamical model of elementary particles based on an analogy with superconductivity. II. *Phys. Rev.* **1961**, *124*, 246–254. [[CrossRef](#)]
37. Vogl, U.; Weise, W. The Nambu and Jona-lasinio model: Its implications for hadrons and nuclei. *Prog. Part. Nucl. Phys.* **1991**, *27*, 195–272. [[CrossRef](#)]
38. Hatsuda, T.; Kunihiro, T. QCD phenomenology based on a chiral effective lagrangian. *Phys. Rep.* **1994**, *247*, 221–367. [[CrossRef](#)]
39. Rehberg, P.; Klevansky, S.P.; Hüfner, J. Hadronization in the SU (3) Nambu–Jona-Lasinio model. *Phys. Rev. C* **1996**, *53*, 410–429. [[CrossRef](#)]
40. Buballa, M. NJL-model analysis of dense quark matter. *Phys. Rep.* **2005**, *407*, 205–375. [[CrossRef](#)]
41. Volkov, M.K.; Radzhabov, A.E. The Nambu–Jona-Lasinio model and its development. *Phys. Uspekhi* **2006**, *49*, 551–562. [[CrossRef](#)]

42. Menezes, D.P.; Providência, C. Warm stellar matter with deconfinement: Application to compact stars. *Phys. Rev. C* **2003**, *68*, 035804. [[CrossRef](#)]
43. Shovkovy, I.; Hanauske, M.; Huang, M. Nonstrange hybrid compact stars with color superconducting matter. *Phys. Rev. D* **2003**, *67*, 103004. [[CrossRef](#)]
44. Klähn, T.; Blaschke, D.; Sandin, F.; Fuchs, C.; Faessler, A.; Grigorian, H.; Röpke, G.; Trümper, J. Modern compact star observations and the quark matter equation of state. *Phys. Lett. B* **2007**, *654*, 170–176.
45. Wang, P.; Thomas, A.W.; Williams, A.G. Phase transition from hadronic matter to quark matter. *Phys. Rev. C* **2007**, *75*, 045202. [[CrossRef](#)]
46. Alford, M.; Sedrakian, A. Compact stars with sequential QCD phase transitions. *Phys. Rev. Lett.* **2017**, *119*, 161104. [[CrossRef](#)]
47. Alaverdyan, G.B.; Vartanyan, Y.L. Hybrid stars in the framework of the local Nambu–Jona-Lasinio model for quark matter. *Astrophysics* **2018**, *61*, 483–498. [[CrossRef](#)]
48. Ranea-Sandoval, I.F.; Orsaria, M.G.; Malfatti, G.; Curin, D.; Mariani, M.; Contrera, G.A.; Guilera, O.M. Effects of hadron-quark phase transitions in hybrid stars within the NJL model. *Symmetry* **2019**, *11*, 425. [[CrossRef](#)]
49. Li, J.J.; Sedrakian, A.; Alford, M. Relativistic hybrid stars with sequential first-order phase transitions and heavy-baryon envelopes. *Phys. Rev. D* **2020**, *101*, 063022. [[CrossRef](#)]
50. Pereira, R.C.; Costa, P.; Providência, C. Two-solar-mass hybrid stars: A two model description using the Nambu–Jona-Lasinio quark model. *Phys. Rev. D* **2016**, *94*, 094001. [[CrossRef](#)]
51. Pais, H.; Menezes, D.P.; Providência, C. Neutron stars: From the inner crust to the core with the (extended) Nambu–Jona-Lasinio model. *Phys. Rev. C* **2016**, *93*, 065805. [[CrossRef](#)]
52. Wu, X.; Ohnishi, A.; Shen, H. Quark matter symmetry energy effect on equation of state for neutron stars. *AIP Conf. Proc.* **2019**, *2127*, 020032.
53. Blaschke, D.; Schaffner-Bielich, J.; Schulze, H.-J. Topical issue on exotic matter in neutron stars. *Eur. Phys. J. A* **2016**, *52*, 71. [[CrossRef](#)]
54. Baym, G.; Hatsuda, T.; Kojo, T.; Powell, P.D.; Song, Y.; Takatsuka, T. From hadrons to quarks in neutron stars: A review. *Rep. Prog. Phys.* **2018**, *81*, 056902. [[CrossRef](#)] [[PubMed](#)]
55. Singh, S.K.; Biswal, S.K.; Bhuyan, M.; Patra, S.K. Effects of  $\delta$  mesons in relativistic mean field theory. *Phys. Rev. C* **2014**, *89*, 044001. [[CrossRef](#)]
56. 'tHooft, G. Symmetry breaking through Bell-Jackiw anomalies. *Phys. Rev. Lett.* **1976**, *37*, 8–11.
57. Masuda, K.; Hatsuda, T.; Takatsuka, T. Hadron-quark crossover and massive hybrid stars with strangeness. *Astrophys. J.* **2013**, *764*, 12. [[CrossRef](#)]
58. Wu, X.H.; Shen, H. Finite-size effects on the hadron-quark phase transition in neutron stars. *Phys. Rev. C* **2017**, *96*, 025802. [[CrossRef](#)]
59. Logoteta, D.; Providência, C.; Vidana, I. Formation of hybrid stars from metastable hadronic stars. *Phys. Rev. C* **2013**, *88*, 055802. [[CrossRef](#)]
60. Lutz, M.; Klimt, S.; Weise, W. Meson properties at finite temperature and baryon density. *Nucl. Phys. A* **1992**, *542*, 521–558. [[CrossRef](#)]
61. Biernat, E.P.; Gross, F.; Peña, M.T.; Stadler, A.; Leitão, S. Quark mass function from a one-gluon-exchange-type interaction in Minkowski space. *Phys. Rev. D* **2018**, *98*, 114033. [[CrossRef](#)]
62. Walecka, J.D. A theory of highly condensed matter. *Ann. Phys.* **1974**, *83*, 491–529. [[CrossRef](#)]
63. Serot, B.D.; Walecka, J.D. The relativistic nuclear many-body problem. In *Advances in Nuclear Physics*; Negele, J.W., Vogt, E., Eds.; Plenum Press: New York, NY, USA, 1986; Volume 16.
64. Serot, B.D.; Walecka, J.D. Recent progress in quantum hydrodynamics. *Int. J. Mod. Phys. E* **1997**, *6*, 515–631. [[CrossRef](#)]
65. Alaverdyan, G.B. Relativistic mean-field theory equation of state of neutron star matter and a Maxwellian phase transition to strange quark matter. *Astrophysics* **2009**, *52*, 132–150. [[CrossRef](#)]
66. Glendenning, N.K. First-order phase transitions with more than one conserved charge: Consequences for neutron stars. *Phys. Rev. D* **1992**, *46*, 1274–1287. [[CrossRef](#)] [[PubMed](#)]
67. Seidov, Z.F. The stability of a star with a phase change in general relativity theory. *Sov. Astron. A J.* **1971**, *15*, 347–348.